Dual role of the coactivator TORC2 in modulating hepatic glucose output and insulin signaling

Gianluca Canettieri,[1,3,4] Seung-Hoi Koo,[1,2,4] Rebecca Berdeaux,[1] Jose Heredia,[1] Susan Hedrick,[1] Xinmin Zhang,[1] and Marc Montminy[1,*]

[1]The Salk Institute for Biological Studies, 10010 North Torrey Pines Road, La Jolla, California 92037
[2]Department of Molecular Cell Biology, Sungkyunkwan University School of Medicine, Suwon 440-746, Korea
[3]Present address: Department of Experimental Medicine and Pathology, University of Rome, "La Sapienza" Viale Regina Elena, 32400161 Rome, Italy
[4]These authors have contributed equally to this manuscript.
*Correspondence: montminy@salk.edu

Summary

Under fasting conditions, the cAMP-responsive CREB coactivator TORC2 promotes glucose homeostasis by stimulating the gluconeogenic program in liver. Following its nuclear translocation in response to elevations in circulating glucagon, TORC2 regulates hepatic gene expression via an association with CREB on relevant promoters. Here, we show that, in parallel with their effects on glucose output, CREB and TORC2 also enhance insulin signaling in liver by stimulating expression of the insulin receptor substrate 2 (IRS2) gene. The induction of hepatic IRS2 during fasting appears critical for glucose homeostasis; knockdown of hepatic IRS2 expression leads to glucose intolerance, whereas hepatic IRS2 overexpression attenuates the gluconeogenic program and reduces fasting glucose levels. By stimulating the expression of IRS2 in conjunction with gluconeogenic genes, the CREB:TORC2 pathway thus triggers a feedback response that limits glucose output from the liver during fasting.

Introduction

Fasting and caloric restriction (CR) have been shown to extend lifespan and to improve energy balance in a wide variety of organisms. CR enhances glucose homeostasis in part by improving insulin sensitivity, although the underlying mechanism is unclear (Bartke and Brown-Borg, 2004; Escalante-Pulido et al., 2003; Heilbronn and Ravussin, 2003).

Under fasting conditions, elevations in pancreatic glucagon trigger the expression of the gluconeogenic program via the cAMP-responsive factor CREB (Mayr and Montminy, 2001; Shaywitz and Greenberg, 1999). Mice deficient in hepatic CREB activity, either via targeted disruption of the CREB gene or by expression of a dominant-negative CREB polypeptide called A-CREB (Ahn et al., 1998), display fasting hypoglycemia and reduced expression of gluconeogenic genes (Herzig et al., 2001).

In a recent study, we found that glucagon stimulates CREB activity via induction of the coactivator TORC2 (Conkright et al., 2003a; Iourgenko et al., 2003; Koo et al., 2005; Screaton et al., 2004). Sequestered in the cytoplasm via a phosphorylation-dependent interaction with 14-3-3 proteins in the fed state, TORC2 is rapidly dephosphorylated and translocated to the nucleus in response to fasting signals, where it stimulates the gluconeogenic program via a direct interaction with CREB. Knockdown of hepatic TORC2 profoundly reduces glucose output and gluconeogenic gene expression in mice (Koo et al., 2005). Indeed, TORC2 overexpression strongly induces glucose output in primary hepatocytes exposed to cAMP agonist. But TORC2 has more modest effects on circulating glucose levels when expressed at similar levels in liver in vivo, suggesting the presence of counter-regulatory controls that feed back on this pathway and protect against fasting hyperglycemia.

Previous studies showing that the cAMP pathway promotes insulin signaling in pancreatic islets by stimulating expression of insulin receptor substrate 2 (IRS2) gene (Jhala et al., 2003) prompted us to examine whether TORC2 limits glucose output from the liver by regulating hepatic IRS2 expression in parallel with the gluconeogenic program during fasting. We found that cAMP triggers IRS2 expression and enhances insulin signaling in hepatocytes via a CREB/TORC2-dependent mechanism. Indeed, acute disruption of hepatic IRS2 expression led to fasting hyperglycemia as well as elevated expression of the gluconeogenic program. The induction of IRS2 by TORC2 thus limits glucose output from the liver and may explain the well-recognized effects of acute caloric restriction in enhancing insulin sensitivity.

Results

The importance of IRS2 in regulating glucose output from liver (Kido et al., 2000; Kubota et al., 2000; Withers et al., 1998) prompted us to examine the dynamics of IRS2 expression relative to the feeding/fasting transition. Levels of hepatic IRS2 mRNA and protein increased robustly during fasting, declining to near undetectable levels during ad libitum feeding or refeeding conditions (Figure 1A). By contrast, levels of IRS1 and insulin receptor appeared relatively constant throughout, suggesting that fasting signals specifically induce IRS2 expression.

We evaluated the importance of IRS2 induction during fasting for glucose homeostasis by acute knockdown of hepatic IRS2 expression with an adenovirus IRS2 RNAi construct (Ad-

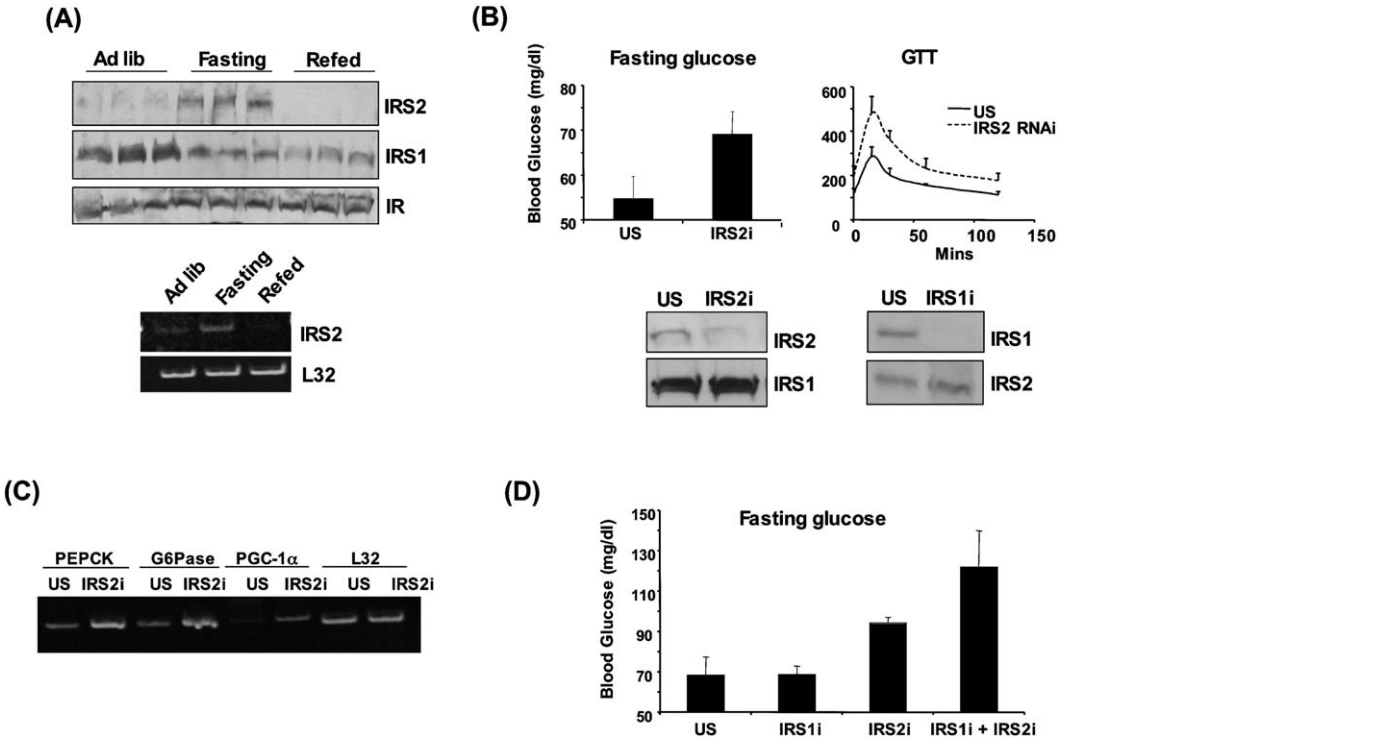

Figure 1. Induction of IRS2 in liver during fasting is required for glucose homeostasis

A) Top, Western blot analysis of hepatic IRS2 protein levels under ad libitum feeding, fasted, and refed conditions. Levels of insulin receptor (IR) and IRS1 shown for comparison. Bottom, PCR analysis of hepatic IRS2 mRNA levels under ad libitum feeding, fasted, and refed conditions.

B) Effect of acute hepatic IRS2 knockdown on fasting glucose metabolism. Top-left, circulating glucose levels in mice (n = 5) infected for 4 days with unspecific (Ad-USi) or IRS2 siRNA-expressing adenovirus. Top-right, glucose tolerance test of Ad-USi and Ad-IRS2i mice (n = 5). Following intraperitoneal injection with glucose (2g/kg), glucose levels were monitored at time points indicated. Bottom, Western blot analysis of IRS1 and IRS2 proteins in livers from mice infected with unspecific control (US), Ad-IRS1i, or Ad-IRS2i RNAi adenoviruses.

C) PCR analysis of gluconeogenic gene (PEPCK, G6P, PGC-1α) expression in livers of control Ad-USi and Ad-IRS2i-expressing mice collected under fasted conditions. L32 mRNA levels shown as control.

D) Effect of hepatic Ad-IRS1i and Ad-IRS2i mediated knockdown, alone or in combination, on fasting glucose levels relative to control Ad-USi mice (n = 4).

Data in (**B**) and (**D**) are represented as mean ± standard deviation.

IRS2i) (Figure 1B). Compared with control littermates, Ad-IRS2i mice exhibited higher fasting blood glucose levels as well as marked glucose intolerance in response to intraperitoneal glucose administration (Figure 1B). Indeed, gluconeogenic gene expression (PEPCK, G6P, PGC-1α) during fasting was increased in IRS2 knockdown relative to control littermates (Figure 1C).

To determine the relative contributions of hepatic IRS1 and IRS2 in this regard, we prepared an Ad- IRS1 RNAi construct (Figure 1B). By contrast with Ad-IRS2i, Ad-IRS1i mice showed no change in fasting glucose levels relative to control littermates (Figure 1D). Nevertheless, mice expressing both Ad-IRS1i andAd-IRS2i showed higher fasting glucose levels compared with Ad-IRS2i mice, indicating that IRS1 is capable of compensating to some extent for the loss of IRS2 signaling (Figure 1D).

Hepatic IRS2 expression is often reduced in mouse models of Type II diabetes, reflecting in part the inhibitory effects of hyperinsulinemia on expression of the IRS2 gene (Brady, 2004; White, 2003). Correspondingly, levels of hepatic IRS2 protein were dramatically lower in *db/db* diabetic relative to control mice, whereas amounts of IRS1 remained comparable between the two groups (Figure 2A). To test whether restoring IRS2 expression is sufficient to promote normoglycemia in a diabetic animal model, we injected *db/db* mice with Ad-IRS2. Relative to control Ad-GFP littermates, Ad-IRS2 mice showed a progressive decline in circulating glucose concentrations during fasting, reaching near normal levels (100 mg/dl) 8 days postinfection (Figure 2B). Ad-IRS2 also enhanced insulin sensitivity in *db/db* mice, as determined by intraperitoneal glucose tolerance test; and levels of circulating insulin were correspondingly reduced by nearly 70% in IRS2 compared to control littermates (Figure 2B, bottom panel; Figure 2C). Similar effects of Ad-IRS2 on glucose tolerance were also obtained with wild-type mice (not shown).

Insulin regulates hepatic metabolism by stimulating a cascade of lipid kinases that culminate in the phosphorylation and activation of the Ser/Thr kinase Akt/PKB (Brazil and Hemmings, 2001). We tested whether hepatic Ad-IRS2 expression was sufficient to potentiate Akt activation and to enhance Ser9 phosphorylation of GSK3, a downstream target of Akt. Compared with control Ad-GFP littermates, liver extracts from Ad-

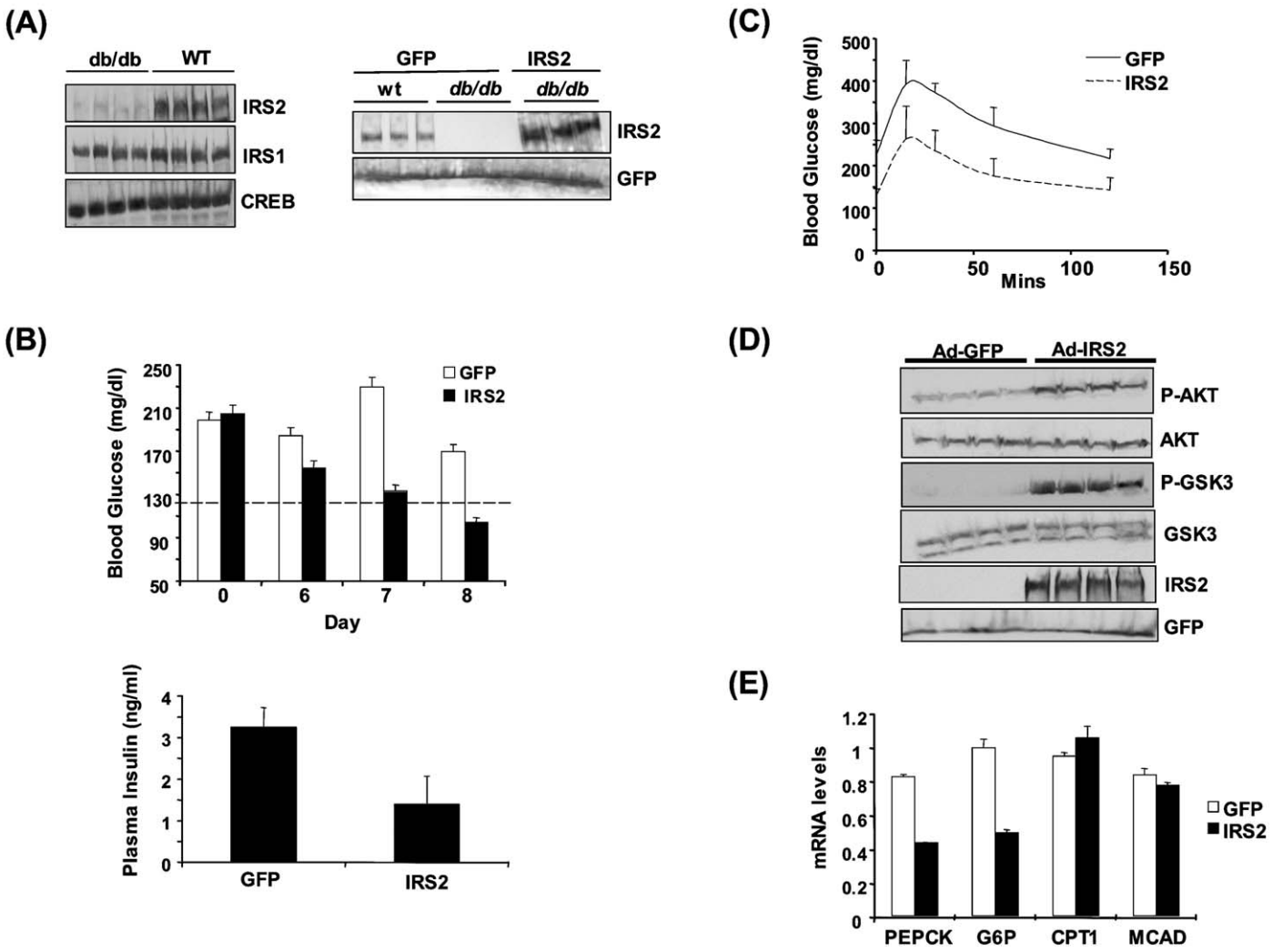

Figure 2. Hepatic IRS2 promotes glucose homeostasis by reducing expression of the gluconeogenic program in liver during fasting

A) Western blot assay of liver extracts from fasted wild-type and *db/db* diabetic mice showing levels of CREB, IRS1, and IRS2. Right, Western blot assay of fasting hepatic IRS2 levels in *db/db* mice infected with Ad-GFP or Ad-IRS2 relative to wild-type Ad-GFP infected mice.

B) Top, fasting glucose levels in *db/db* mice infected with Ad-GFP or Ad-IRS2 adenovirus. Days after infection are indicated. Stippled line indicates normal fasting glucose levels. Bottom, circulating insulin levels in Ad-GFP and Ad-IRS2 *db/db* mice collected under fasting conditions. Plasma insulin levels were determined 8 days postinfection (n = 5).

C) Glucose tolerance test of *db/db* mice infected with Ad-GFP or Ad-IRS2 adenovirus (n = 5). Plasma glucose levels were determined at time points indicated (in min) after IP injection of glucose (2 g/kg).

D) Effect of IRS2 expression on insulin signaling in livers of *db/db* diabetic mice. Levels of total and phospho (Ser473) Akt as well as amounts of total and phospho (Ser9)GSK3β are shown for four different mice.

E) Effect of Ad-IRS2 infection on gluconeogenic gene expression in fasted *db/db* mice. Q-PCR analysis of hepatic PEPCK and G6Pase mRNA levels after normalizing to L32 gene expression in Ad-GFP and Ad-IRS2 *db/db* mice (n = 4).

Data in (**B**), (**C**), and (**E**) are represented as mean ± standard deviation.

IRS2 mice contained far higher amounts of phospho (Ser473) Akt and phospho (Ser9) GSK3 by Western blot assay (Figure 2D). In keeping with these effects, gluconeogenic gene expression was markedly reduced in IRS2 expressing *db/db* mice, demonstrating that IRS2 promotes glucose homeostasis, in part by disrupting expression of the gluconeogenic program (Figure 2E).

The ability of fasting signals to stimulate IRS2 expression led us to examine the role of CREB in this process. The mouse IRS2 promoter contains a consensus CRE at –671 (Jhala et al., 2003). In gel mobility shift assays, a double-stranded oligo containing the IRS2 CRE was found to bind CREB family members CREB-1 and CREM (data not shown, Figure 3A). Binding of CREM to the IRS2 CRE sequence was readily disrupted by adding 50-fold molar excess unlabeled wild-type but not mutant CRE oligonucleotide, demonstrating that the binding of CREB family members to this site is indeed specific.

Consistent with CRE binding studies, exposure of HepG2 hepatocytes to FSK stimulated a wild-type IRS2 luciferase reporter 7-fold but had no effect on mutant IRS2 reporter con-

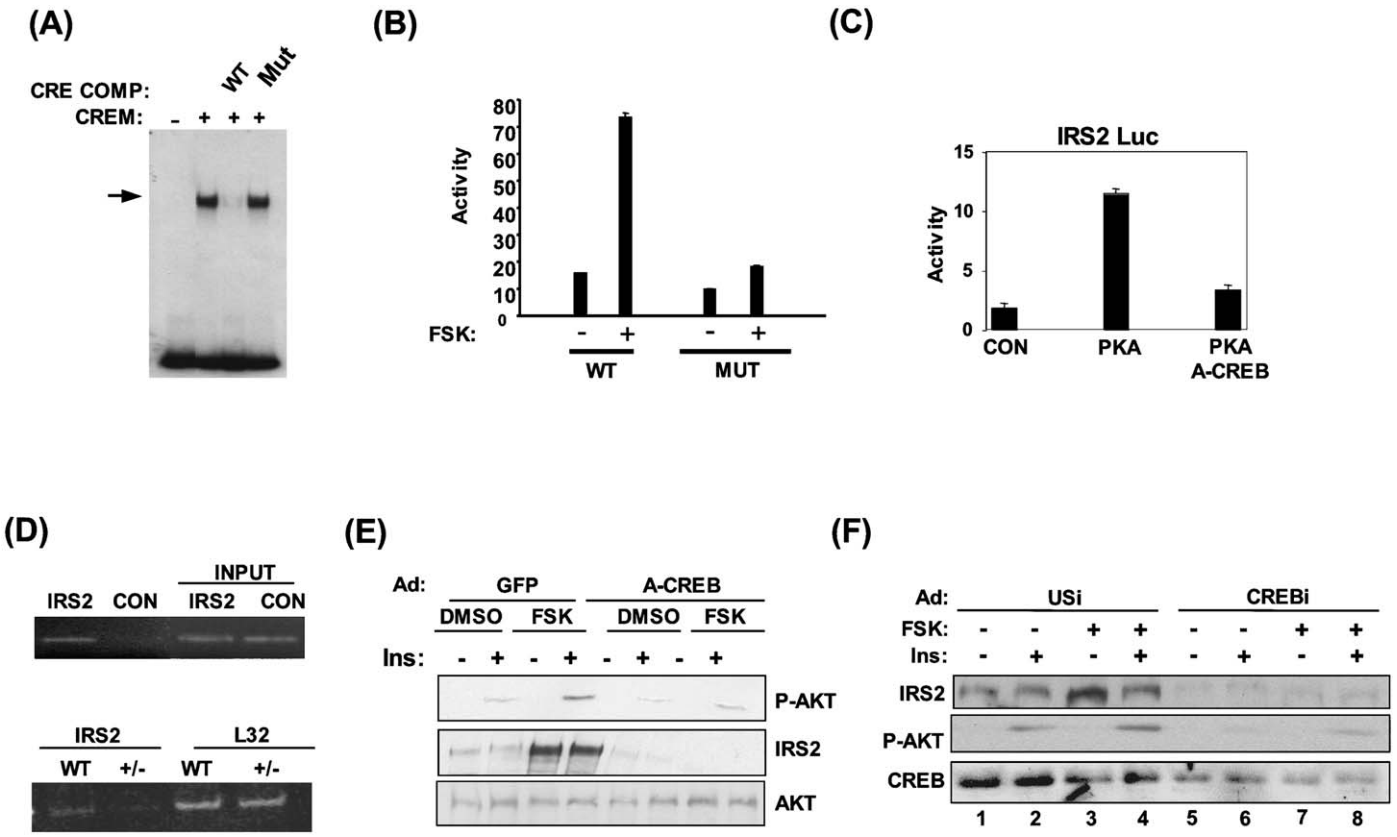

Figure 3. Fasting signals promote hepatic IRS2 expression via the cAMP-responsive factor CREB

A) Gel mobility shift assay of ^{32}p-labeled CRE oligonucleotide from the IRS-2 promoter. Incubation of recombinant CREM with 50-fold molar excess unlabeled wild-type (WT) and mutant (CRE) CRE oligonucleotide competitors shown.

B) Transient assays of mouse hepatocytes transfected with IRS2-luciferase reporter constructs. Effect of FSK on activity of wild-type and CRE mutant IRS2 promoter constructs.

C) Effect of CREB dominant-negative polypeptide (A-CREB) on IRS-2 reporter activity in cells transfected with PKA expression vector. Luciferase activity was normalized to cotransfected RSV-β galactosidase activity.

D) Top, chromatin immunoprecipitation (ChIP) assay showing recovery of PCR-amplified IRS2 promoter fragment from immunoprecipitates of CREB prepared from mouse hepatocytes. Absence of control ACTB (CON) promoter fragment in CREB immunoprecipitates shown to confirm specificity of the CREB antiserum. Bottom, PCR analysis of hepatic IRS2 mRNA levels in CREB$^{+/-}$ mice compared to control littermates under fasted conditions. mRNA levels for the constitutively expressed L32 gene are also shown.

E) Effect of cAMP/CREB pathway in promoting insulin signaling in hepatocytes. Top, primary cultures of rat hepatocytes were infected with dominant-negative A-CREB or control GFP adenovirus for 48 hr and then exposed to FSK or DMSO vehicle for 8 hr. Effect of subsequent short-term (30 min) insulin treatment on Ser473 phosphorylation of Akt under various conditions shown by Western blot assay. Levels of total Akt and IRS2 protein also indicated.

F) Western blot showing effect of Ad-CREB RNAi or unspecific (USi) RNAi adenovirus (3 day infection) on IRS2 levels in primary rat hepatocytes. Effect of insulin treatment (30 min.) on AKT Ser473 phosphorylation indicated. Prior treatment with FSK (4 hr) shown.

Data in (**B**) and (**C**) are represented as mean ± standard deviation.

taining substitutions within the CRE that block CREB binding (Figure 3B). Indeed, overexpression of the catalytic subunit for the cAMP-dependent protein kinase A (PKA) enhanced IRS2 promoter activity 10-fold; and these effects were disrupted by expression of a dominant-negative polypeptide A-CREB (Ahn et al., 1998), which blocks the DNA binding activity of CREB family members (CREB-1, CREM, ATF-1) but not other bZIP transcription factors (Figure 3C).

In chromatin immunoprecipitation (ChIP) assays of mouse hepatocytes, the IRS2 promoter was efficiently recovered from CREB immunoprecipitates whereas a control (ACTB) promoter lacking a consensus CRE site was not (Figure 3D, top). Indeed, hepatic IRS2 mRNA levels were reduced in fasted CREB$^{+/-}$ knockout mice compared to wild-type littermates (Figure 3D, bottom). Taken together, these experiments reveal that the IRS2 gene is indeed a direct target of CREB action in hepatocytes.

Having seen that fasting signals trigger expression of the IRS2 gene via a CREB-dependent mechanism, we examined whether these effects are propagated at the level of IRS2 protein accumulation. Exposure of primary rat hepatocytes to FSK-induced IRS2 protein levels gradually over a 6–12 hr period; and the accumulation of IRS2 protein was completely suppressed either by blocking cellular CREB activity with Ad-A-CREB (Figure 3E) or by reducing endogenous CREB expression with Ad-CREB RNAi (Figure 3F).

The ability of CREB to promote IRS2 mRNA and protein accumulation in response to cAMP agonist led us to consider

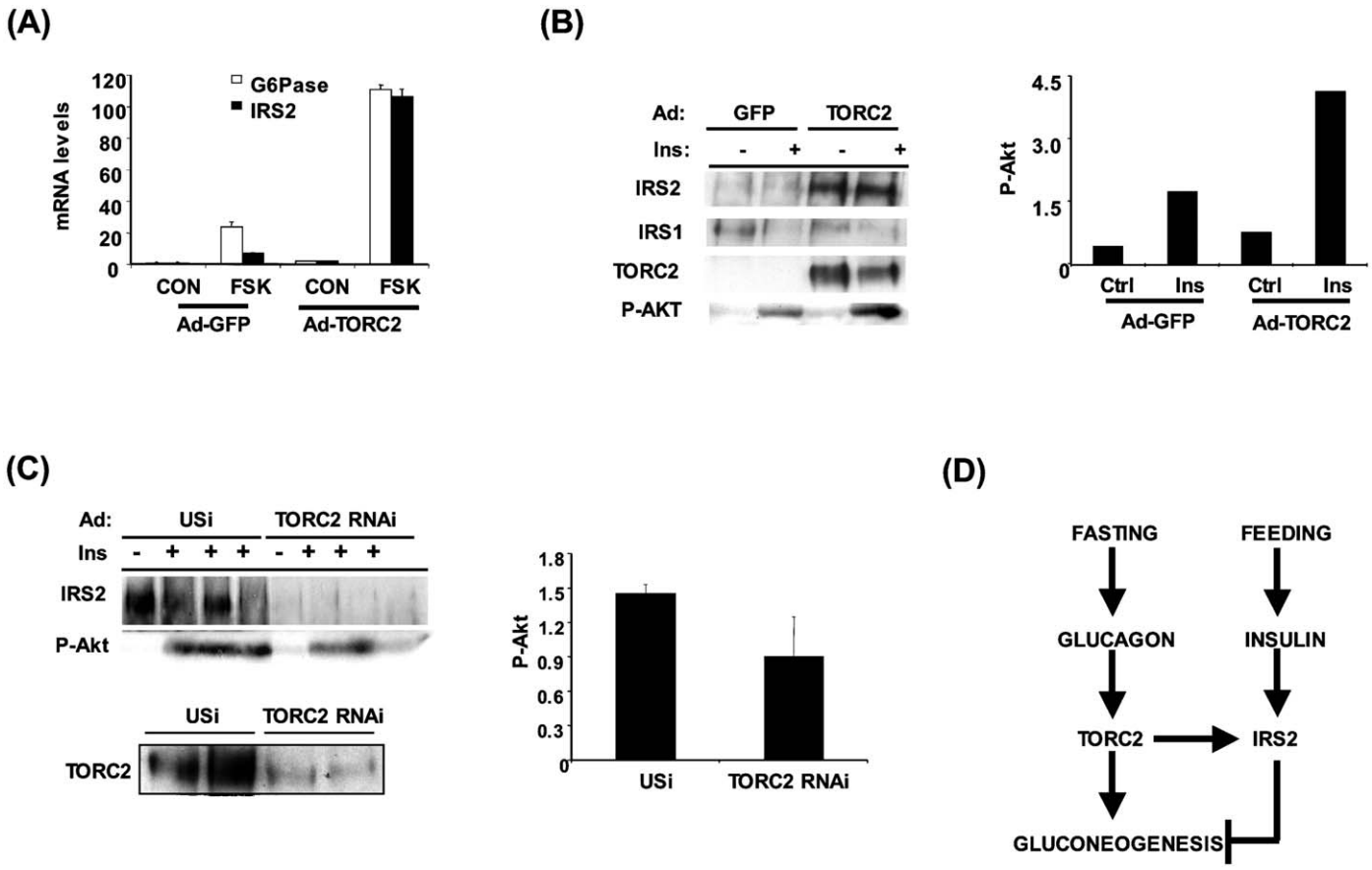

Figure 4. The CREB coactivator TORC2 promotes hepatic IRS2 expression and enhances insulin signaling in vivo

A) Effect of Adenoviral TORC2 relative to control GFP adenovirus on IRS2 mRNA levels in primary rat hepatocytes. Glucose 6 phosphatase mRNA levels shown for comparison. Treatment with FSK indicated.

B) Left, Western blot assays showing effect of Ad-TORC2 expression in primary hepatocytes on IRS2 protein levels and on insulin-dependent phosphorylation of Akt at Ser473. IRS1 and TORC2 levels are also shown. Treatment with insulin (30 min) indicated. Right, bar graph showing relative levels of phospho (Ser473) Akt in Ad-GFP or Ad-TORC2 hepatocytes exposed to insulin (30 min), as measured by densitometric analysis.

C) Effect of intraperitoneal insulin treatment (10 min.) on hepatic Ser473 phosphorylation of Akt in Ad-USi and Ad-TORC2i mice. Western blot assay of liver extracts showing amounts of IRS2 and Phospho (Ser473) Akt in both groups. Treatment with insulin is indicated. Bottom, levels of TORC2 protein in Ad-USi and Ad-TORC2i livers. Right, relative levels of phospho (Ser473)Akt in liver extracts from Ad-USi and Ad-TORC2i mice, measured by densitometric analysis.

D) Model for TORC2 action in liver. Under fasting conditions, TORC2 stimulates hepatic glucose output via induction of gluconeogenic genes in response to pancreatic glucagon. In parallel, TORC2 protects against hyperglycemia by stimulating expression of IRS2 and thereby enhancing insulin signaling.

Data in (**A**) and (**C**) are represented as mean ± standard deviation.

whether this pathway enhances insulin signaling and potentiates activation of downstream effectors like Akt/PKB. Consistent with its effects on IRS2 accumulation, FSK pretreatment (8 hr) increased Ser473 phosphorylation of Akt in response to short-term exposure (30 min) to insulin (Figure 3E). Conversely, hepatocytes deficient in CREB activity due either to Ad-A-CREB expression (Figure 3E) or to knockdown of CREB with Ad-CREB RNAi construct (Figure 3F) were far less responsive to insulin treatment.

Having seen that CREB promotes insulin signaling by stimulating IRS2 expression, we sought to determine the mechanism underlying these effects. The importance of the CREB coactivator TORC2 for induction of the gluconeogenic program during fasting (Koo et al., 2005) prompted us to evaluate its role in IRS2 activation. Following exposure to FSK, Ad-TORC2 increased amounts of IRS2 mRNA to a similar extent (10-fold) as the gluconeogenic Glucose 6 Phosphatase (G6Pase) gene in primary hepatocytes (Figure 4A). Correspondingly, Ad-TORC2 also enhanced accumulation of IRS2 protein but had no effect on IRS1 levels. Indeed, Ad-TORC2 expressing hepatocytes were 2- to 3-fold more responsive to acute insulin stimulation, as determined by Akt phosphorylation (Figure 4B).

To determine whether TORC2 is required for IRS2 expression and insulin signaling in liver, we injected mice with an adenovirus TORC2 RNAi construct (Ad-TORC2 RNAi). Compared with control mice injected with an unspecific RNAi adenovirus (Ad-USi), Ad-TORC2 RNAi mice exhibited markedly lower TORC2 protein levels by Western blot assay (Figure 4C, bottom). Correspondingly, IRS2 protein was almost undetectable in liver extracts from Ad-TORC2 RNAi mice, confirming the importance of this coactivator in mediating induction of the IRS2 gene during fasting (Figure 4C, top). Ad-TORC2 RNAi mice were also

less responsive to insulin; following intraperitoneal injection of insulin (10 min), the accumulation of phospho (Ser473) Akt in Ad-TORC2 RNAi mice was reduced 2-fold compared to control mice (Figure 4C). Taken together, these results suggest that the coordinate induction of IRS2 and gluconeogenic genes by TORC2 provides important feedback controls that ensure against fasting hyperglycemia due to excessive hepatic glucose output (Figure 4D).

Discussion

TORC2 has been shown to promote hepatic glucose output during fasting by stimulating expression of the gluconeogenic program in response to glucagon (Koo et al., 2005). By contrast with its robust activity in primary hepatocytes, TORC2 has more modest effects on gluconeogenesis when expressed in liver. We found that fasting signals also enhance IRS2 gene expression via the CREB:TORC2 pathway. The induction of IRS2 potentiates insulin signaling in primary hepatocytes, as revealed by enhanced phosphorylation of Akt in response to acute insulin stimulation. Conversely, knockdown of hepatic IRS2 expression led to fasting hyperglycemia with elevated expression of gluconeogenic genes, pointing to an important role for IRS2 in limiting glucose output in the fasted state.

TORC2 and CREB are likely to regulate IRS2 expression in concert with other transcriptional regulators, most notably the forkhead protein FOXO1 (Ide et al., 2004). Indeed, forkhead proteins have also been found to exert priming effects on insulin signaling; Tjian and colleagues found that *Drosophila* FOXO (dFOXO) strongly induced expression of the insulin receptor (IR) gene by binding to conserved FOXO responsive elements in the dIR promoter (Puig et al., 2003). Thus, in addition to constraining glucose output, fasting signals may prepare certain tissues for the transition to feeding by upregulating components of the insulin signaling pathway.

By contrast with IRS2, hepatic IRS1 expression did not differ between fasting and feeding periods; and acute knockdown of IRS1 had little effect on fasting glucose levels. These results are consistent with previous gene disruption studies showing that IRS1 promotes insulin signaling primarily in skeletal muscle (Araki et al., 1994; Tamemoto et al., 1994). Our results differ from those reported by Kahn and colleagues, who recently observed greater effects of IRS-1 relative to IRS-2 on gluconeogenic gene expression in their knockdown experiments (Taniguchi et al., 2005). The reasons for this discrepancy are unclear but may reflect differences in knockdown efficiency.

The notion that IRS2 performs a critical role in liver glucose metabolism during fasting is further supported by Ad-IRS2 overexpression experiments in *db*/*db* diabetic mice, which exhibit low levels of hepatic IRS2 but not IRS1. The loss of IRS2 expression during feeding and in *db*/*db* mice is likely to reflect combined effects of hyperinsulinema on IRS2 protein recycling and degradation as well as on transcriptional regulation by Foxo family members (Rui et al., 2002; Shi et al., 2004). Indeed, modest overexpression of IRS2 was sufficient to reduce fasting glucose levels and gluconeogenic gene expression to near normal levels in *db*/*db* mice.

Exercise and short-term caloric restriction have been shown to improve insulin sensitivity in peripheral tissues (Bartke and Brown-Borg, 2004; Escalante-Pulido et al., 2003; Heilbronn and Ravussin, 2003). Based on its ability to potentiate insulin signaling, TORC2 may contribute to the salutary effects of CR on glucose homeostasis in liver and perhaps other tissues. Future studies in lower organisms like *Drosophila* may reveal whether TORC2 also mediates certain effects of CR on longevity.

Experimental procedures

Plasmids

The pXp2 IRS-2 luciferase reporter vector, the expression vectors for PKAc, and A-CREB were described previously (Herzig et al., 2003, 2001). To generate pU6-IRS2 RNAi and pU6-IRS1 RNAi constructs, palindromic sequences corresponding to nucleotides 258–280 from mouse IRS2 coding sequence (5′-GGGCGCGCCGAAGCGAGTGATC-3′) and nucleotides 936–957 from mouse IRS1 coding sequence (5′–GGGTGGGAAACCAGGTTC CTTC-3′) were linked to human U6 promoter in the pBluescript KS vector. The unspecific control was described elsewhere (Koo et al., 2004). To generate FLAG IRS2, the coding sequence of mouse IRS2 was PCR amplified from the His IRS2 vector (kindly provided by Morris White) and subcloned into FLAG pCDNA3 (Conkright et al., 2003b).

Culture of primary hepatocytes

Rat primary hepatocytes were prepared from 200–300 g of Sprague-Dawley rats by collagenase perfusion method as described previously (Koo et al., 2004). 1×10^6 cells were plated in 6-well plates with medium 199 (Invitrogen, Carlsbad, California) supplemented by 10% FBS, 10 units/ml penicillin, 10 μg/ml streptomycin, and 10 nM dexamethasone for 3–6 hr. After attachment, cells were infected with adenoviruses expressing either GFP or A-CREB, TORC2, or CREB RNAi, for 16 hr. Subsequently, cells were maintained in medium 199 without FBS and dexamethasone for 8 hr, treated with 10 μM forskolin or DMSO for 8 hr, and then with 100 nM insulin for 30 min.

Transfection assays

Human hepatoma HepG2 cells were maintained with Ham's F12 medium supplemented with 10% FBS (Invitrogen, Carlsbad, California). For transfection, Fugene 6 reagent (Promega, Madison, Wisconsin) was used according to the manufacturer's instructions. Each transfection was performed with 50 ng of luciferase construct, 25 ng of β galactosidase expression plasmid, and 25 ng each of expression vector for PKAc and A-CREB. Luciferase activity was normalized to β galactosidase activity (Jhala et al., 2003).

Recombinant adenoviruses

Adenoviruses expressing GFP only, A-CREB, and unspecific control were described previously (Herzig et al., 2001; Koo et al., 2004). Adenoviruses were generated by homologous recombination between adenovirus backbone vector pAD-Easy and linearized transfer vector pAD-Track that contains U6-IRS1 RNAi, U6-IRS2 RNAi, and CMV-FLAG IRS2 cDNA, respectively. For animal experiments, viruses were purified on a CsCl gradient and then dialyzed against PBS buffer containing 10% glycerol, prior to injection.

Animal experiments

Male 7-week-old C57BL6 mice and *db*/*db* mice were purchased from the Jackson Laboratory and maintained on regular chow under a 12 hr light-dark cycle. 0.5×10^9 plaque-forming units per recombinant adenovirus were delivered by systemic tail vein injection to mice that were anaesthetized with Iso-Flurane. For measuring fasting blood glucose level, animals were fasted for 16 hr with free access to water. Blood glucose was monitored at the end of each fasting period. Liver tissues were collected at the end of experiments and immediately frozen in liquid nitrogen. Sections of liver samples were fixed in 10% formaldehyde and analyzed under the fluorescence microscope to determine infection efficiency. RNA was isolated using Trizol solution (Invitrogen, Carlsbad, California), and liver RNAs, collected from three mice within each experimental group, were pooled for quantitative PCR analysis.

Glucose tolerance test

Mice were fasted for 16 hr prior to the glucose tolerance test and then injected intraperitoneally with 2 g/kg body weight of glucose (Herzig et al.,

2001; Koo et al., 2004). Blood glucose levels were measured from tail vein blood collected at designated times.

Measurement of metabolites

Blood glucose levels were monitored from tail vein blood using an automatic glucose monitor (One Touch, Lifescan, Fremont, California). Plasma insulin levels were determined using a commercial insulin enzyme-linked immunosorbent assay kit (Crystal Chem, Chicago, Illinois).

Quantitative PCR

Total RNA from either primary hepatocytes or liver tissue was extracted using RNeasy mini-kit (Qiagen, Valencia, California). 500 ng (for primary hepatocytes) or 1 μg (for mouse liver) of total RNA was used for generating cDNA with Superscript II enzyme (Invitrogen, Carlsbard, California). cDNAs were analyzed by quantitative PCR using SYBR green PCR kit and an AB-IPRISM 7700 Sequence detector (Perkin Elmer, Foster City, California). All PCR data were normalized to ribosomal L32 expression in the corresponding sample.

Western blotting

Whole cell protein was extracted from liver tissue in SDS-urea-lysis buffer. 50–100 μg of protein was loaded onto a 6% SDS-polyacrylamide gel and blotted onto nitrocellulose membrane (Schleicher & Schuell, Keene, New Hampshire). Western blot assays were performed as described. Antisera against IRS1 and IRS2 were from Upstate. Antibodies against Akt and GSK-3β were purchased from Cell Signaling (Boston, Massachusetts).

Acknowledgments

We thank members of the Montminy laboratory for helpful discussions. This work was supported by National Institutes of Health grant GM RO1-37828, by the Hillblom Foundation, and by the Keickhefer Foundation. G.C. is a recipient of a Juvenile Diabetes Research Foundation fellowship award and S.-H.K. is supported by an American Diabetes Association training fellowship award.

Received: December 28, 2004
Revised: July 29, 2005
Accepted: September 20, 2005
Published: November 8, 2005

References

Ahn, S., Olive, M., Aggarwal, S., Krylov, D., Ginty, D., and Vinson, C. (1998). A dominant negative inhibitor of CREB reveals that it is a general mediator stimulus-dependent transcription of c-fos. Mol. Cell. Biol. *18*, 967–977.

Araki, E., Lipes, M.A., Patti, M.E., Bruning, J.C., Haag, B., 3rd, Johnson, R.S., and Kahn, C.R. (1994). Alternative pathway of insulin signalling in mice with targeted disruption of the IRS-1 gene. Nature *372*, 186–190.

Bartke, A., and Brown-Borg, H. (2004). Life extension in the dwarf mouse. Curr. Top. Dev. Biol. *63*, 189–225.

Brady, M.J. (2004). IRS2 takes center stage in the development of type 2 diabetes. J. Clin. Invest. *114*, 886–888.

Brazil, D.P., and Hemmings, B.A. (2001). Ten years of protein kinase B signalling: a hard Akt to follow. Trends Biochem. Sci. *26*, 657–664.

Conkright, M.D., Canettieri, G., Screaton, R., Guzman, E., Miraglia, L., Hogenesch, J.B., and Montminy, M. (2003a). TORCs: transducers of regulated CREB activity. Mol. Cell *12*, 413–423.

Conkright, M.D., Guzmán, E., Flechner, L., Su, A.I., Hogenesch, J., and Montminy, M. (2003b). Genome wide analysis of CREB target genes reveals a core promoter requirement for cAMP responsiveness. Mol. Cell *11*, 1101–1108.

Escalante-Pulido, M., Escalante-Herrera, A., Milke-Najar, M.E., and Alpizar-Salazar, M. (2003). Effects of weight loss on insulin secretion and in vivo insulin sensitivity in obese diabetic and non-diabetic subjects. Diabetes Nutr. Metab. *16*, 277–283.

Heilbronn, L.K., and Ravussin, E. (2003). Calorie restriction and aging: review of the literature and implications for studies in humans. Am. J. Clin. Nutr. *78*, 361–369.

Herzig, S., Hedrick, S., Morantte, I., Koo, S.H., Galimi, F., and Montminy, M. (2003). CREB controls hepatic lipid metabolism through nuclear hormone receptor PPAR-gamma. Nature *426*, 190–193.

Herzig, S., Long, F., Jhala, U., Hedrick, S., Quinn, R., Bauer, A., Schutz, G., Yoon, C., Puisgever, P., Spiegelman, B., and Montminy, M. (2001). CREB regulates hepatic gluconeogenesis via the co-activator PGC-1. Nature *413*, 179–183.

Ide, T., Shimano, H., Yahagi, N., Matsuzaka, T., Nakakuki, M., Yamamoto, T., Nakagawa, Y., Takahashi, A., Suzuki, H., Sone, H., et al. (2004). SREBPs suppress IRS-2-mediated insulin signalling in the liver. Nat. Cell Biol. *6*, 351–357.

Iourgenko, V., Zhang, W., Mickanin, C., Daly, I., Jiang, C., Hexham, J.M., Orth, A.P., Miraglia, L., Meltzer, J., Garza, D., et al. (2003). Identification of a family of cAMP response element-binding protein coactivators by genome-scale functional analysis in mammalian cells. Proc. Natl. Acad. Sci. USA *100*, 12147–12152.

Jhala, U.S., Canettieri, G., Screaton, R.A., Kulkarni, R.N., Krajewski, S., Reed, J., Walker, J., Lin, X., White, M., and Montminy, M. (2003). cAMP promotes pancreatic beta-cell survival via CREB-mediated induction of IRS2. Genes Dev. *17*, 1575–1580.

Kido, Y., Burks, D.J., Withers, D., Bruning, J.C., Kahn, C.R., White, M.F., and Accili, D. (2000). Tissue-specific insulin resistance in mice with mutations in the insulin receptor, IRS-1, and IRS-2. J. Clin. Invest. *105*, 199–205.

Koo, S.H., Flechner, L., Qi, L., Zhang, X., Screaton, R., Jeffries, S., Hedrick, S., Xu, W., Boussouar, F., Brindle, P., et al. (2005). The CREB coactivator TORC2 is a key regulator of fasting glucose metabolism. Nature *437*, 1109–1111.

Koo, S.H., Satoh, H., Herzig, S., Lee, C.H., Hedrick, S., Kulkarni, R., Evans, R.M., Olefsky, J., and Montminy, M. (2004). PGC-1 promotes insulin resistance in liver through PPAR-alpha-dependent induction of TRB-3. Nat. Med. *10*, 530–534.

Kubota, N., Tobe, K., Terauchi, Y., Eto, K., Yamauchi, T., Suzuki, R., Tsubamoto, Y., Komeda, K., Nakano, R., Miki, H., et al. (2000). Disruption of insulin receptor substrate 2 causes type 2 diabetes because of liver insulin resistance and lack of compensatory beta-cell hyperplasia. Diabetes *49*, 1880–1889.

Mayr, B., and Montminy, M. (2001). Tanscriptional regulation by the phosphorylation dependent factor CREB. Nat. Rev. Mol. Cell Biol. *2*, 599–609.

Puig, O., Marr, M.T., Ruhf, M.L., and Tjian, R. (2003). Control of cell number by Drosophila FOXO: downstream and feedback regulation of the insulin receptor pathway. Genes Dev. *17*, 2006–2020.

Rui, L., Yuan, M., Frantz, D., Shoelson, S., and White, M.F. (2002). SOCS-1 and SOCS-3 block insulin signaling by ubiquitin-mediated degradation of IRS1 and IRS2. J. Biol. Chem. *277*, 42394–42398.

Screaton, R.A., Conkright, M.D., Katoh, Y., Best, J.L., Canettieri, G., Jeffries, S., Guzman, E., Niessen, S., Yates, J.R., 3rd, Takemori, H., et al. (2004). The CREB coactivator TORC2 functions as a calcium- and cAMP-sensitive coincidence detector. Cell *119*, 61–74.

Shaywitz, A.J., and Greenberg, M.E. (1999). CREB: a stimulus-induced transcription factor activated by a diverse array of extracellular signals. Annu. Rev. Biochem. *68*, 821–861.

Shi, H., Tzameli, I., Bjorbaek, C., and Flier, J.S. (2004). Suppressor of cytokine signaling 3 is a physiological regulator of adipocyte insulin signaling. J. Biol. Chem. *279*, 34733–34740.

Tamemoto, H., Kadowaki, T., Tobe, K., Yagi, T., Sakura, H., Hayakawa, T., Terauchi, Y., Ueki, K., Kaburagi, Y., Satoh, S., et al. (1994). Insulin resistance

and growth retardation in mice lacking insulin receptor substrate-1. Nature *372*, 182–186.

Taniguchi, C.M., Ueki, K., and Kahn, R. (2005). Complementary roles of IRS-1 and IRS-2 in the hepatic regulation of metabolism. J. Clin. Invest. *115*, 718–727.

White, M.F. (2003). Insulin signaling in health and disease. Science *302*, 1710–1711.

Withers, D.J., Gutierrez, J.S., Towery, H., Burks, D.J., Ren, J.M., Previs, S., Zhang, Y., Bernal, D., Pons, S., Shulman, G.I., et al. (1998). Disruption of IRS-2 causes type 2 diabetes in mice. Nature *391*, 900–904.